

Self-Compensation of PZT Errors in White Light Scanning Interferometry

Min-Gu Kang, Sang-Yoon Lee and Seung-Woo Kim*

*Department of Mechanical Engineering, Korea Advanced Institute of Science and Technology
Taejon 305-701, KOREA*

(Received February 23, 1999)

One of main error sources in white light scanning interferometry is the inaccuracy of scanning mechanisms in that PZT (piezoelectric transducer) micro-actuators are preferably used. We propose a new calibration method that is capable of identifying actual scanning errors directly by analyzing the spectral distribution of sampled interferograms. This calibration provides an effective means of self-compensation for the non-linearity errors caused by PZT hysteresis, enhancing the measurement uncertainty to a level of 5 nanometers over an entire measuring range of 100 μm .

I. INTRODUCTION

White light scanning interferometry produces short coherence interferograms whose fringe visibility is narrowly localized, so that the optical path difference between the test and reference beams can be precisely scaled without 2π -ambiguity. During the last two decades much attention has been paid to three-dimensional surface mapping using white light scanning interferometry. As a result, quite a few sophisticated techniques have been well established to achieve extremely fine measuring resolutions typically in the nanometer regime [1]. However, the measuring uncertainty is significantly affected by non-linear errors caused by PZT hysteresis, and it is usually far worse than the resolution in proportion with required measuring range. One fortunate fact is that PZT hysteresis is so systematic that it can be well predicted if the operating input condition is known [2]. It is consequently common in practice to drive PZT actuators following a predefined upward path in that the input voltage is increased from the zero state. The output displacement in this case becomes repeatable and its systematic non-linear behavior with the input voltage can be well predicted and subsequently compensated using pre-calibrated step artifacts [3].

One practical problem with using a step artifact is the pre-calibration uncertainty that is usually in the range of a few nanometers. For accurate compensation, the step height of the artifact needs to be made as small as possible so that the detailed non-linear response of the PZT ceramics to the input voltage is

characterized step by step over the entire operating range. In doing that, however, the pre-calibration error tends to accumulate as the compensation proceeds and reaches to a significant level in the end. Now, to cope with the problem, this paper proposes a new calibration method in which no accumulation of pre-calibration error occurs. This method basically allows a self-calibration in that actual scanning intervals are identified directly from sampled interferograms. The key idea is that the spectral distribution of the white light involved in scanning interferometry can be readily computed by transforming interferograms into the spectral domain [4]. Then the central wavenumber is identified as the centroid of the spectral distribution and, directly related with the scanning step intervals actually used in measurement. This technique needs the pre-calibrated artifact only once when the physical dimension of the central wavenumber is determined. In addition, the step height of the artifact can be made large enough to be about the size of the whole scanning range, so that averaging effects minimizing the uncertainty in deciding the central wavenumber can be obtained.

II. CENTRAL WAVENUMBER

White light scanning interferometry for three-dimensional surface mapping can be performed with a variety of optical setups such as Michelson, Mirau, and Linnik interferometers. A Mirau type configuration shown in Fig. 1 is taken here in its simplest form to explain working principles of white light scanning interferometry. Interferograms are sampled using a

*Who is responsible for correspondence and correction.

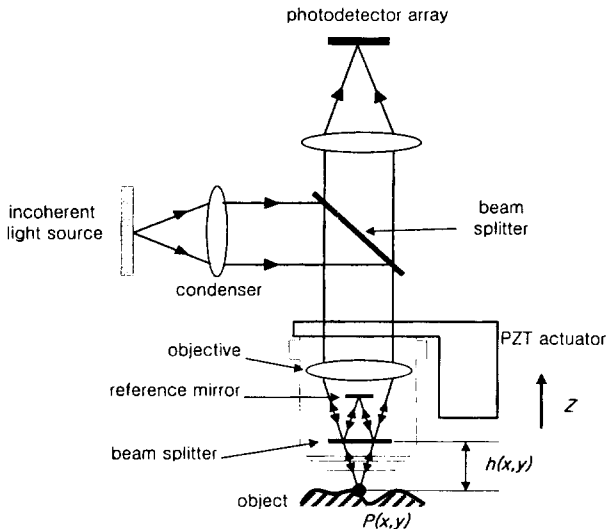


FIG. 1. Optical configuration of the Mirau interferometer.

photodetector array while moving the target surface along the z direction using a PZT actuator. At a point $P(x, y)$ on the surface whose height is $h(x, y)$, its scanning interferogram may be considered as the incoherent superposition of individual scanning interferograms of monochromatic waves such as [5]

$$I(z) = I_0 + \int F(k) \cos [2k(h - z) + \alpha] dk \quad (1)$$

where I_0 is the mean intensity, $k = \frac{2\pi}{\lambda}$, and $F(k)$ represents the spectral distribution of white light involved in interference. The phase shift of light occurring upon reflection from the surface is called α , which is regarded here as a constant for simplicity of analysis. The result of performing the integral operation of Eq. (1) depends upon the detailed profile of $F(k)$, and it may be approximated as [1]

$$I(z) = I_0 + a(h - z) \cos (2k_c(h - z) + \alpha) \quad (2)$$

where k_c denotes the central wavenumber, while $a(h - z)$ is referred to as the visibility envelop function. Fig. 2 shows a typical interferogram that is obtained from a Tungsten-Halogen lamp, whose temporal coherence length measures about $4 \mu\text{m}$. Interference fringes are narrowly localized in the spatial domain due to short coherence, being wrapped by the visibility envelop function $a(h - z)$. The analytical expression of $a(h - z)$ usually turns out to be a Gaussian or sinc type function for most practically available light sources [5].

Whatever the actual shape of $a(h - z)$ is, it is noted that the function $a(h - z)$ always holds the property of

$$a(0) = \int F(k) dk. \quad (3)$$

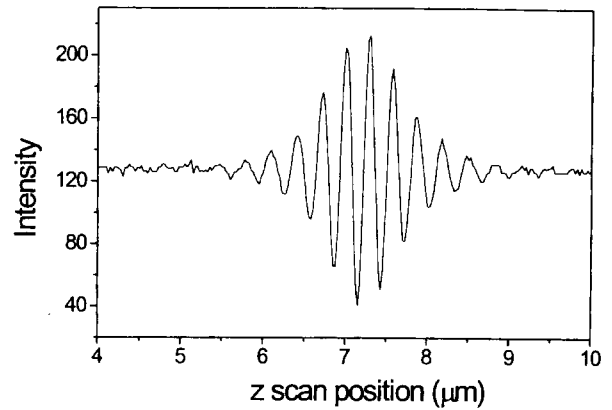


FIG. 2. A typical interferogram from tungsten-halogen lamps ($N.A. = 0.4$).

This can be easily verified by substituting $z = h$ into Eqs. (1) and (2). In addition, differentiating Eqs. (1) and (2), and substituting $z = h$ again give the intermediate result of

$$-2 \int k F(k) \sin \alpha dk = \frac{\partial a(h - z)}{\partial z} \Big|_{z=h} \cos \alpha - 2k_c a(0) \sin \alpha. \quad (4)$$

In the above, the first differential term in the right hand side is always zero since the function $a(h - z)$ is supposed to be at its maximum when $z = h$. Consequently, combining Eq. (3) with Eq. (4) yields a useful relationship of

$$k_c = \frac{\int k F(k) dk}{\int F(k) dk}. \quad (5)$$

This result implies that the central wavenumber k_c defined in Eq. (2) in fact corresponds to the centroid abscissa of the spectral distribution $F(k)$.

The spectral distribution $F(k)$ as defined in Eq. (1) demands some deliberation to precisely understand how it should be determined. It is apparent that the primary contribution to $F(k)$ is the emitted spectrum of the light source in use. In addition, since it is to be attributed to the interference fringes finally sampled, $F(k)$ is supposed to be influenced by the reflectance of the test surface and also by the optical transmittance of the lenses involved in interferometry and the spectral sensitivity of the photodetector array being used. Therefore $F(k)$ is not faithfully indicated solely by the spectral distribution of the light source itself that can be measured with a well-calibrated spectrometer. In other words, $F(k)$ has to be identified directly from sampled interferograms. Eq. (1) notes that when the measured intensity I_z is transformed into the spectral domain, the resulting spectral amplitude straightforwardly stands for $F(k)$ [4]. Fig. 3 shows an exemplary result of $F(k)$, which was computed by Fourier trans-

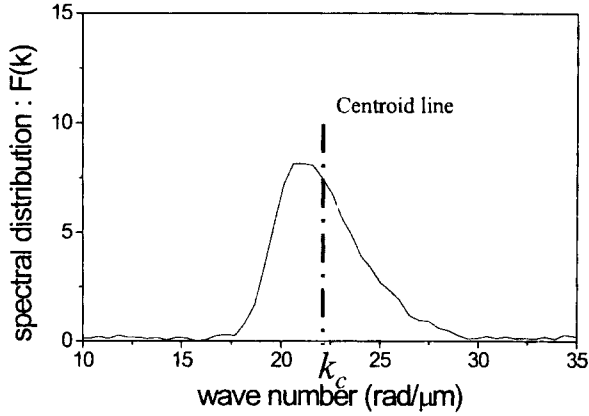


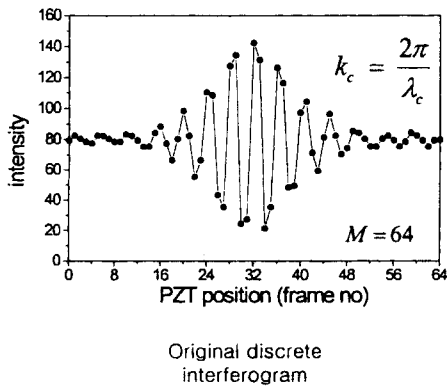
FIG. 3. The spectral distribution of a tungsten-halogen lamp.

forming the interferogram obtained from a tungsten-halogen lamp. Accordingly, once the distribution of $F(k)$ is computed, the central wavenumber k_c can then be determined as the centroid abscissa following Eq. (5), as illustrated in the figure.

III. CALIBRATION

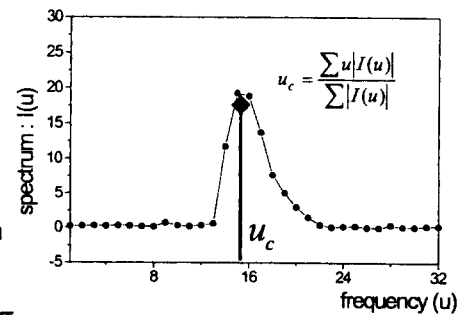
For calibration of PZT scanning errors, it becomes necessary to find the relationship between the computed central wavenumber k_c and the step interval Δz that is to be used in actual scanning. Discrete Fourier transforming is adopted in determining $F(k)$, so let's assume that a whole interferogram is sampled by collecting a total of M discrete intensity data points while being successively scanned by the step interval Δz . Then the z -coordinate is expressed in discrete form as $z_i = z_0 + i \cdot \Delta z$, where $i = 0, 1, 2, \dots, M-1$. And the discrete Fourier transform of $I(z)$ of Eq. (1) is performed as

$$I(u) = \sum_{i=0}^{M-1} I(z_i) \exp \left[\frac{-j2\pi u i}{M} \right]$$



Discrete Fourier transform

$$2k_c = \frac{2\pi}{M\Delta z} u_c$$



Spectral distribution

FIG. 4. Relationship between the central wavenumber and centroid abscissa in the spectral domain.

$$\text{for } u = 0, 1, 2, \dots, \frac{M}{2}. \quad (6)$$

where u indicates the index number of spatial frequency. The frequency interval of the discretely transformed $I(u)$ is determined as $\Delta \nu = 1/(M\Delta z)$, while the spatial frequency is given as $\nu = u/(M\Delta z)$. Now, using the relationship of Eq. (5), the central frequency ν_c can be readily decided as $\nu_c = u_c/(M\Delta z)$, where u_c specifically corresponds to the centroid abscissa of $I(u)$. If the Mirau interferometer concerned is of reflection type, the optical path becomes twice the scanning distance, i.e., $2k_c = 2\pi\nu_c = (2\pi/M\Delta z)u_c$. Accordingly, as illustrated in Fig. 4, the scanning step interval is finally related with the central wavenumber k_c such as

$$\Delta z = \kappa \cdot u_c \quad (7)$$

where κ now becomes a constant expressed as $\kappa = \pi/Mk_c$. This result shows that the scanning step interval Δz can be identified from the centroid abscissa u_c of the Fourier transformed data of $I(z)$, provided the central wavenumber k_c is known.

The relationship of Eq. (7) can be used for compensation of PZT errors with the calibration scheme configured in Fig. 5. The PZT actuator under calibration is to move a Mirau type microscope objective in the scanning range of 0 to 100 μm . The voltage

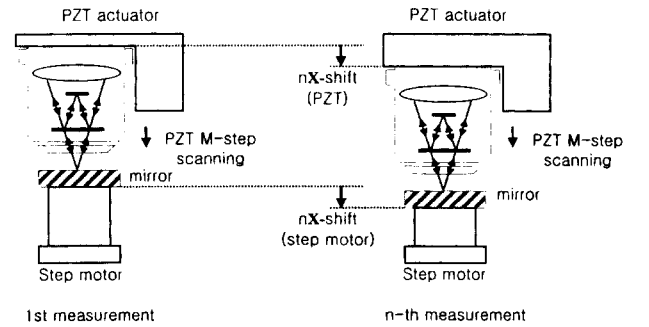


FIG. 5. Calibration scheme of PZT hysteresis errors.

input to the actuator varies from 0 to 100 V with a mean sensitivity of 1.0 $\mu\text{m}/\text{V}$. A flat mirror is placed on a specimen table, whose vertical position is raised in sequence using a stepping motor with a predetermined increment of 5 μm typically. At each vertical position of the specimen table, scanning interferograms are sampled against the flat mirror by driving the PZT actuator with a scanning step interval of 80 nm. This calibration scheme provides exactly alike interferometric conditions regardless of vertical positions of the specimen table. An identical spectral condition is consequently maintained in all the measurements of scanning interferograms, so that the central wavenumber k_c remains unchanged.

Fig. 6 shows a series of interferograms, which were actually sampled with an incremental interval of 10 μm over the whole PZT scanning range of 100 μm . It is not surprising that the sampled interferograms are unlike with different fringe periods, indicating actual scanning step intervals are not the same due to PZT hysteresis. Accordingly, the centroid abscissa u_c of Eq. (7) varies with the input voltage, so it may be expressed as

$$u_c(V) = \sum_{n=0}^N c_n V^n \quad (8)$$

where c_n represents the polynomial coefficients to be fitted. Numerical values of u_c are computed using Eq. (5) every 5 μm along the whole PZT range. Then using least squares technique the coefficients c_n are determined so that a complete description of u_c is constructed in terms of the input voltage V in a polynomial form.

Now, in order to identify the constant κ that contains the central wavenumber k_c , a new variable $U_c(V)$ is defined such as

$$U_c(V) = \int_0^V u_c(V) dV = \sum_{n=0}^N \frac{c_n}{n+1} V^{n+1} \quad (9)$$

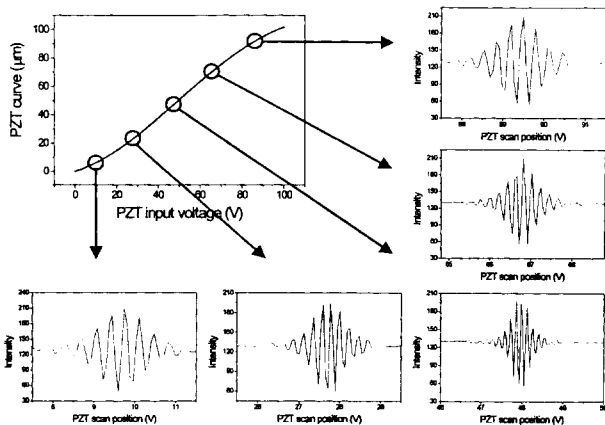


FIG. 6. Interferograms at different PZT scanning positions.

which is referred to as the accumulated centroid index. Once the polynomial of $u_c(V)$ is obtained, $U_c(V)$ can be readily determined using the coefficients c_n . Let us assume that a known step height H is measured, then it can be expressed as

$$H = \int_{V_1}^{V_2} \Delta z(V) dV = \kappa \int_{V_1}^{V_2} u_c(V) dV = \kappa [U_c(V_2) - U_c(V_1)] \quad (10)$$

in which V_1 and V_2 denote the initial and final input voltages where the bottom and upper surfaces of the step height are detected, respectively. Since the accumulated centroid index has been previously obtained as a point function in terms of input voltage V , the constant κ is attained as $\kappa = H/[U_c(V_2) - U_c(V_1)]$. The accurate value of H should be known through a precise pre-calibration means such as a standard laser interferometer used for gauge blocks calibration. In performing the pre-calibration, it is important to note that the step height H should be taken as large as possible to be about the size of the whole scanning range. The reason is that some calibration error is inevitable in determining H , even though it is usually limited to a few nanometers. Thus the uncertainty in H is averaged in the computed κ through a large value of $[U_c(V_2) - U_c(V_1)]$.

Fig. 7 shows the experimental result in which the values of scanning step intervals were computed with the calibrated κ using the relationship of Eq. (7). In fact, scanning step intervals were commanded to be 80 nm, but their induced values were in the range from 60 to 85 nm. The solid curve exhibited in the figure represents the fitted result in which up to the ninth polynomials were used, i.e., $N = 9$. Now Fig. 8 displays the full path of the PZT actuator, which was obtained as

$$z(V) = \int_0^V \Delta z(V) dV$$

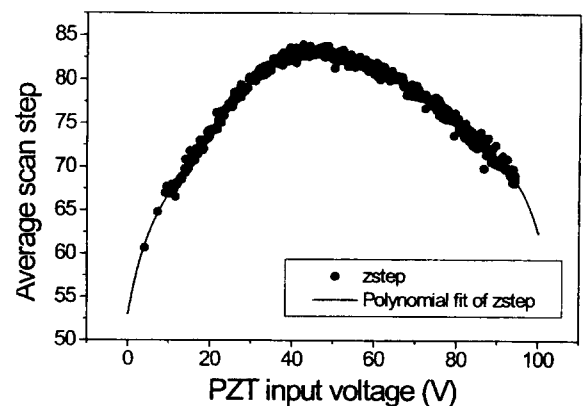


FIG. 7. Measured step intervals.

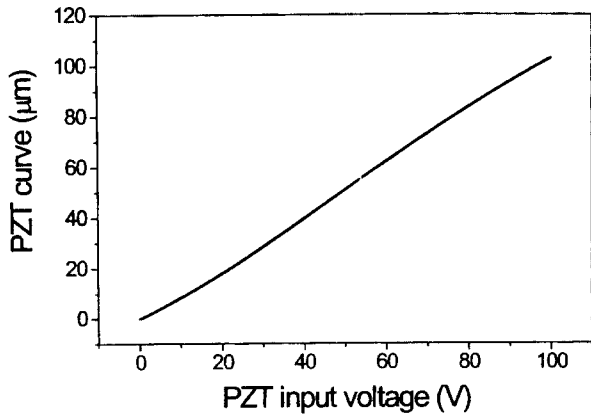


FIG. 8. Measured PZT response curve.

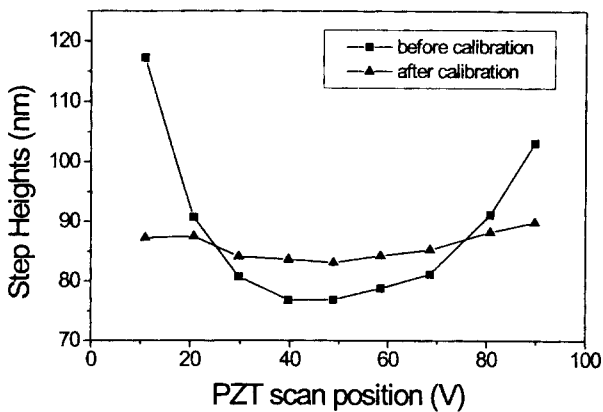


FIG. 9. Measurement results of an identical step height.

$$= \kappa \int_0^V u_c(V) dV \equiv \kappa \cdot U_c(V) . \quad (11)$$

The experimental result clearly shows the PZT hysteresis effects causing measurement inaccuracy.

Finally, a standard step height of 84 nm was repeatedly measured at various positions over the whole operating range of the PZT actuator. As shown in Fig.

9, when no calibration was made, the measured height values vary from 75 to 97 nm depending upon the operating position of the actuator. On the other hand, when calibration was done, the measured height values have a small variation of less than 4 nm over the entire operating range. In addition, the maximum standard deviation of the measured heights is found within 2 nanometers, which were verified through 30 consecutive measurements at every calibration position. In this test, a white light phase-measuring algorithm that is performed in three consecutive steps was used. As illustrated in Fig. 10, in the first step of the algorithm, the envelope function is extracted using the Hilbert transform [6] on the 64 intensity data point sampled from a scanning interferogram. Then, in the second step, the intensity data are simultaneously offset to have a mean of zero, and divided by the computed envelope function to obtain a purely sinusoidal intensity pattern. In the final third step, a group of 15 intensity data points is selected around the envelope peak point, and the true fringe peak point is precisely determined relying upon a phase-shifting technique that has well been established in coherent laser interferometry. Once the compensation of PZT scanning errors has been done, the actual scanning interval of the chosen 15 data points is not found to be accurately either $\pi/2$ or $\pi/3$ even though intended as such. Therefore, a least-squares phase-measuring algorithm that can well work with an unequally-spaced intensity data set was used to find the relative phase of the true fringe peak [7].

IV. CONCLUSION

In this investigation, a self-compensation method of PZT errors in white light scanning interferometry has been presented. The method identifies actual scanning errors directly by analyzing the spectral distribution of sampled interferograms. This technique needs the

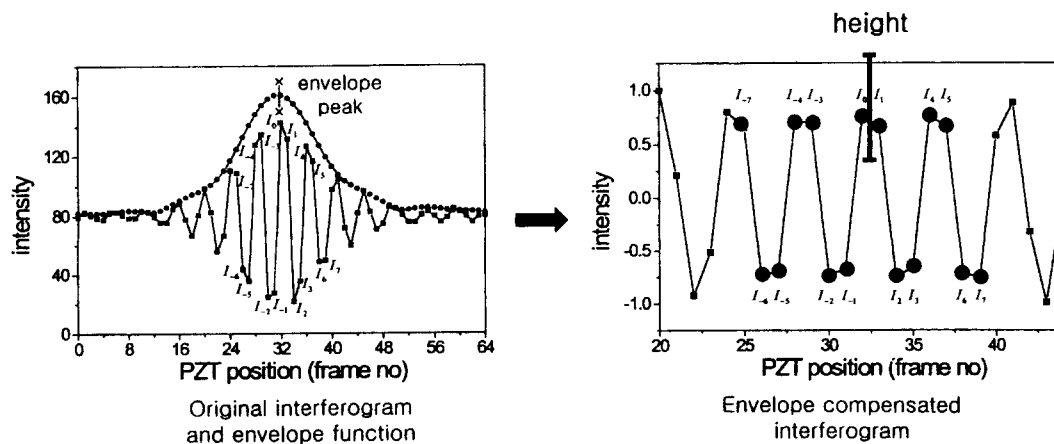


FIG. 10. The white light phase-measuring algorithm for peak detection.

pre-calibrated artifact only once when the physical dimension of the central wavenumber is determined. In addition, the step height of the artifact can be made large enough to be about the size of the whole scanning range, so that averaging effects minimizing the uncertainty in deciding the central wavenumber can be obtained. Experimental results prove that a PZT scanning error of about 25 nm can be reduced to a level of 4 nm with a repeatability of less than 2 nm.

REFERENCES

- [1] K. Creath, Proc. Fringe '97, 52 (1997).
- [2] S. Kim, S. Jung, Precision Engineering **16**, 49 (1994).
- [3] M. Kanai, W. Gao, I. Ogura, S. Kiyono, Proc. of the ASPE, 414 (1997).
- [4] B. Danielson and C. Boisrobert, Appl. Opt. **30**, 2975 (1991).
- [5] M. Born and E. Wolf, *Principles of Optics* (Pergamon Press, Sixth ed., 1985) p. 316.
- [6] S. Chim and G. Kino, Appl. Opt. **31**, 2550 (1992).
- [7] D. Malacara, *Optical Shop Testing* (Wiley, New York, 2nd ed., 1992) Chapter 14.